

Thermoelectric properties of a ferromagnet-superconductor hybrid junction: Role of interfacial Rashba spin-orbit interaction

Paramita Dutta,^{1,*} Arijit Saha,^{1,2,†} and A. M. Jayannavar^{1,2,‡}

¹*Institute of Physics, Sachivalaya Marg, Bhubaneswar-751005, India*

²*Homi Bhabha National Institute, Training School Complex, Anushakti Nagar, Mumbai 400085, India*

We explore thermal transport phenomena through a ferromagnet-superconductor hybrid structure with Rashba spin-orbit interaction at the interfacial layer. The exponential rise of thermal conductance with temperature manifests a cross-over temperature scale separating the two regimes corresponding to the opposite behaviors of the thermal conductance with the change of polarization in the ferromagnet. Inclusion of finite potential barrier at the ferromagnet-superconductor interface results in reduction of the thermal conductance whereas the interfacial Rashba spin-orbit field can enhance it resulting in a non-monotonic behavior as a function of the Rashba spin-orbit coupling. We employ scattering matrix approach to determine the amplitudes of all the quantum mechanical scattering processes possible at the interface and the thermal conductance therein. We explain the thermoelectric properties of the hybrid structure in terms of different parameters of the system. We also investigate the Seebeck effect and show that higher thermopower can be achieved when the polarization of the ferromagnet tends towards the half-metallic limit. Whereas it can be enhanced even for lower polarization when there is a finite barrier potential at the junction. In presence of Rashba spin-orbit interaction, Seebeck co-efficient rises with the increase of barrier strength and also with the polarization at weak or moderate interfacial Rashba strength. From the application perspective, we also compute the figure of merit which can exceed 1 ($zT \sim 4 - 5$) with higher polarization of the ferromagnet both in absence and presence of weak Rashba spin-orbit interaction.

PACS numbers: 73.23.-b, 74.45.+c, 74.25.fc

I. INTRODUCTION

In comparison to the metallic and semiconducting material, study of thermal transport in superconducting material is less favorable as the thermoelectric effects are strongly suppressed in superconductor^{1,2}. One of the reasons behind this is the interference of temperature dependent super-current with the thermal current. Also the electron-hole symmetry present in the superconducting density of states (DOS) makes the opposite-directional electron and hole thermo-currents generated due to the thermal gradient nullifying each other³.

In recent times, superconducting hybrid structures especially ferromagnet-superconductor (FS) junctions have attracted a lot of research interests due to the dramatic boosts of thermoelectric effects in them¹⁻⁷. Inducing spin-triplet correlation within the superconductor and the asymmetric DOS profiles corresponding to the two spin sub-bands of the ferromagnet are the key features to be utilized in order to make such FS junction suitable in the context of thermal transport. The asymmetry in the two spin sub-bands according to the polarization of the ferromagnet can manipulate the Andreev reflection (AR) which occurs when an incoming electron reflects back as a hole from the FS interface resulting in a cooper pair transmission into the superconductor within the sub-gapped regime⁸.

In order to investigate the thermoelectric properties of a material or hybrid junction it is customary to derive the thermal conductance (TC) or thermal current generated by the temperature gradient⁹⁻¹¹. Particularly in case of superconducting hybrid junction the information

of the superconducting gap parameter like its magnitude, symmetry etc. can be extracted from the behavior of the thermal conductance⁹. From the application perspective it is more favorable to compute the so-called Seebeck co-efficient (SkC), also known as thermopower, which is the open circuit voltage developed across the junction due to the electron flow caused by the thermal gradient¹². Enhancement of SkC can pave the way of promising applications to make an efficient heat-to-energy converter which may be a step forward to the fulfillment of the global demand of energy¹¹. Since last few decades intense research is being carried out in search of newer and efficient energy harvesting devices that convert waste heat into electricity^{13,14}. Usage of good thermoelectric material is one of the ways of making those devices more efficient. Now in order to determine how good thermoelectric a system is, one can calculate SkC as well as the dimensionless parameter called figure of merit (FOM) which is naively the ratio of the power extracted from the device to the power we have to continually provide in order to maintain the temperature difference^{15,16}. It provides us an estimation of the efficiency of a mesoscopic thermoelectric device like refrigerator, generator etc. based on thermoelectric effects¹⁷. Improving this thermoelectric FOM with enhanced SkC is one of the greatest challenges in material science to make the heat-electricity conversion very efficient¹⁸⁻²². Particularly, enhancement of the performance of any superconducting hybrid junction is much more challenging due to the above-mentioned reasons.

The prospects of FS junction, as far as thermoelectric property is concerned, also depends on the new ingredients such as to manipulate the spin dependent particle-

hole symmetry. The latter has been implemented using external magnetic field^{3,7,23–25}, quantum dot at the junction²⁶, non-uniform exchange field²⁷, phase modulation²⁸, magnetic impurities⁴ or internal properties like inverse proximity effect²⁹ etc. Recently, Machon *et al.* have considered simultaneous effects of spin splitting and spin polarized transport² in order to obtain enhanced thermoelectric effects in FS hybrid structure. In addition to these effects, presence of spin-orbit field^{11,23} can also play a vital role in this context.

Study of interfacial spin-orbit coupling effect on transport has become a topic of intense research interest during past few decades due to the spin manipulation³⁰. Interplay of the polarization and the interfacial field may lead to marked anisotropy in the junction electrical conductance³¹ and Josephson current³². Interfacial spin-orbit field, especially Rashba spin-orbit field^{33,34}, arising due to the confinement potential at the semiconductor or superconductor hybrid structure can also be the key ingredient behind such spin manipulation³⁵.

However, the aspect of thermal transport in FS hybrid junction incorporating the role of interfacial spin-orbit interaction remained unexplored so far to the best of our knowledge. A few groups have performed their research in this direction^{10,11}. Motivated by these facts, in this letter we study thermoelectric properties of a FS structure with Rashba spin orbit interaction (RSOI)^{33,36} at the interfacial layer. We employ Blonder-Tinkham-Klapwijk³⁷ (BTK) formalism to compute the TC, SkC and FOM therein. We investigate the role of RSOI on the thermoelectric properties. The interfacial scalar barrier at the FS interface reduces the TC. On the other hand, the presence of RSOI at the FS interface can stimulate enhancement of TC driven by the thermal gradient across the junction. In order to reveal the local thermoelectric response we investigate the behavior of the thermopower with the polarization, temperature as well as the barrier strength. Seebeck co-efficient is enhanced when the polarization of the ferromagnet increases towards the half-metallic limit. In presence of finite barrier strength it could be higher for low polarization also. Presence of RSOI at the interface may reduce or enhance it depending on the barrier strength, temperature and the polarization. For higher barrier strength it always shows non-monotonic behavior with the temperature both in presence and absence of RSOI. Similar non-monotonic behavior is also obtained for FOM with the rise of temperature and Rashba strength. We predict that FOM can exceed the value 1 with higher polarization of the ferromagnet. The magnitude can even be more than 5 for higher strength of barrier potential at the junction. It is also true in presence of weak RSOI. On the contrary, strong Rashba interaction can reduce it irrespective of the polarization and temperature.

The remainder of the paper is organized as follows. In Sec. II we describe our model and the theoretical background. We discuss our results for thermal conductance, thermopower and Figure of merit in Sec. III. Finally, we

summarize and conclude in Sec. IV.

II. MODEL AND THEORETICAL BACKGROUND

We consider a model comprising of a ferromagnet F ($z > 0$) and a s -wave superconductor S ($z < 0$) hybrid structure as shown in Fig. 1. The flat interface of semi-infinite ferromagnet-superconductor (FS) junction located at $z = 0$ is modeled by a δ -function potential with dimensionless barrier strength Z ^{37,38} and Rashba spin-orbit interaction (RSOI) with strength λ_{rso} . The FS junction can be described by the Bogoliubov-deGennes (BdG) equation³⁹ as,

$$\begin{bmatrix} [\hat{H}_e - \mu]\hat{\sigma}_0 & \hat{\Delta} \\ \hat{\Delta}^\dagger & [\mu - \hat{H}_h]\hat{\sigma}_0 \end{bmatrix} \Psi(\mathbf{r}) = E\Psi(\mathbf{r}) \quad (1)$$

where the single-particle Hamiltonian for the electron is given by,

$$\hat{H}_e = -(\hbar^2/2m)\nabla^2 - (\Delta_{xc}/2)\Theta(z)\mathbf{m}\cdot\hat{\sigma} + \hat{H}_{int}. \quad (2)$$

Similarly, for hole the Hamiltonian reads $\hat{H}_h = \hat{\sigma}_2\hat{H}_e^*\hat{\sigma}_2$. The excitations of the electrons with effective mass m are measured with respect to the chemical potential μ . We set $m = 1$ and $\mu = 0$ throughout our calculation. The interface barrier is described by the Hamiltonian $\hat{H}_{int} = (Vd\hat{\sigma}_0 + \omega \cdot \hat{\sigma})\delta(z)$ ³¹ with the height V , width

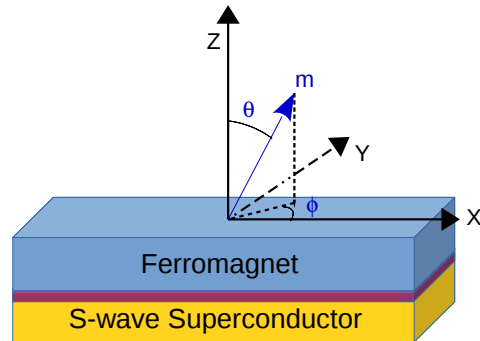


FIG. 1. (Color online) Cartoon of the FS junction with the magnetization vector \mathbf{m} . The dark red color is used to highlight the interfacial region of the FS hybrid structure. The F-region is kept at higher temperature ($T_F = T + \delta T/2$) compared to the S-region ($T_S = T - \delta T/2$) in order to maintain a temperature gradient ($\delta T = T_F - T_S$) across the junction.

d and Rashba field $\omega = \lambda[k_y, -k_x, 0]$, λ being the effective strength of the RSOI. The Stoner band model⁴⁰, characterized by exchange spin splitting Δ_{xc} , is employed to describe the F-region with the magnetization vector $\mathbf{m} = [\sin\theta \cos\phi, \sin\theta \sin\phi, \cos\theta]$. Here $\hat{\sigma}$ is the Pauli spin matrix. Note that, the growth direction (z -axis) of the heterostructure is chosen along [001] crystallographic axis⁴¹. The superconducting pairing potential

is expressed as $\hat{\Delta} = \Delta_s \Theta(z) \sigma_0$ *i.e.* here we assume it to be a spatially independent positive constant following Ref. 31.

Depending on the incoming electron energy there are four scattering processes possible at the FS interface. For electron with a particular spin say, σ , there can be normal reflection (NR), Andreev reflection (AR), tunneling as electron like (TE) or hole like (TH) quasi-particles. In addition to these phenomena there may be spin-flip scattering processes due to the interfacial spin-orbit field. Accordingly, we can have spin-flip counter parts of the above-mentioned four scattering processes namely, spin-flip NR (SNR), spin-flip AR (SAR), spin-flip TE (STE) and spin-flip TH (STH)^{42,43}. The above mentioned scattering processes are schematically displayed in Fig. 2 for

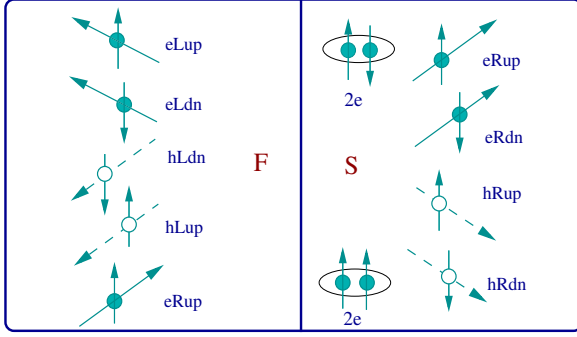


FIG. 2. (Color online) Schematic diagram for the quantum mechanical scattering processes taking place at FS interface. The solid and hollow spheres are used to denote electron (e) and hole (h), respectively. Whereas the letters 'R (L)' indicates the right (left)-moving particles. Corresponding spin states are denoted by 'up' (\uparrow) and 'down' (\downarrow), respectively.

a right-moving electron with spin \uparrow (eRup). Note that, due to the possibility of spin-flip scattering processes in presence of RSOI at the FS interface, spin-triplet⁴⁴ superconducting correlation ($\uparrow\uparrow$ or $\downarrow\downarrow$) can also be induced in addition to the conventional singlet pairing ($\uparrow\downarrow$ or $\downarrow\uparrow$)³¹.

The solution of the BdG equations for the F-region, describing electrons and holes with spin σ , can be written as³¹,

$$\Psi_{\sigma}^F(z) = \frac{1}{\sqrt{k_{\sigma}^e}} e^{ik_{\sigma}^e z} \psi_{\sigma}^e + r_{\sigma,\sigma}^e e^{-ik_{\sigma}^e z} \psi_{\sigma}^e + r_{\sigma,\sigma}^h e^{ik_{\sigma}^e z} \psi_{\sigma}^h + r_{\sigma,-\sigma}^e e^{-ik_{\sigma}^e z} \psi_{-\sigma}^e + r_{\sigma,-\sigma}^h e^{ik_{\sigma}^e z} \psi_{-\sigma}^e \quad (3)$$

where $k_{\sigma}^{e(h)} = \sqrt{k_F^2 - k_{\parallel}^2 + 2m(\sigma\Delta_{xc}/2 + (-)E)/\hbar^2}$ is the electron (hole)-like wave vector. σ may be ± 1 depending on whether the spin is parallel or anti-parallel to the vector \mathbf{m} . k_F and k_{\parallel} are the Fermi and in-plane wave vector, respectively. The spinors for the electron-like and hole-like quasi-particles are respectively $\psi_{\sigma}^e = [\psi_{\sigma}, 0]^T$ and $\psi_{\sigma}^h = [0, \psi_{\sigma}]^T$ with $\psi_{\sigma}^T = [\sigma\sqrt{1 + \sigma \cos \theta} e^{-i\phi}, \sqrt{1 - \sigma \cos \theta}]/\sqrt{2}$. Here, $r_{\sigma,\sigma'}^{e(h)}$ corresponds to the amplitude of normal (Andreev) reflection

from the FS interface. σ and σ' are the spin states for the incident and reflected electron or hole depending on the spin-conserving or spin-flipping process. Similarly, inside the superconducting region the solutions for the electron-like and hole like quasiparticles read³¹

$$\Psi_{\sigma}^S = t_{\sigma,\sigma}^e \begin{bmatrix} u \\ 0 \\ v \\ 0 \end{bmatrix} e^{iq_e z} + t_{\sigma,-\sigma}^e \begin{bmatrix} 0 \\ u \\ 0 \\ v \end{bmatrix} e^{iq_e z} + t_{\sigma,\sigma}^h \begin{bmatrix} u \\ 0 \\ v \\ 0 \end{bmatrix} e^{-iq_h z} + t_{\sigma,-\sigma}^h \begin{bmatrix} 0 \\ u \\ 0 \\ v \end{bmatrix} e^{-iq_h z}, \quad (4)$$

where the z -components of the quasi-particle wave vectors can be expressed as, $q_{e(h)} = \sqrt{q_F^2 - k_{\parallel}^2 + (-)2m\sqrt{E^2 - \Delta^2}/\hbar^2}$ and the superconducting coherence factors are $u(v) = \sqrt{[1 \pm \sqrt{1 - \Delta^2/E^2}]/2}$. We set the Fermi wave vector in both the F and S-regions to be the same *i.e.* $q_F = k_F$ ³¹. Note that, we have written only the z components of the wave functions. In the $x - y$ plane the wave vector is conserved giving rise to the planar wave function as, $\Psi_{\sigma}(\mathbf{r}) = \Psi_{\sigma}(z) e^{i(k_x x + k_y y)}$ where k_x and k_y are the components of k_{\parallel} . Here, $t_{\sigma,\sigma'}^{e(h)}$ denote the amplitude of spin-conserving or spin-flipping transmitted electron (hole) like quasi-particles in the S region. We obtain the reflection and transmission amplitudes using the boundary conditions as,

$$\begin{aligned} \Psi_{\sigma}^F|_{z=0+} &= \Psi_{\sigma}^S|_{z=0-}, \\ \frac{\hbar^2}{2m} \left(\frac{d}{dz} \Psi_{\sigma}^S|_{z=0-} - \frac{d}{dz} \zeta \Psi_{\sigma}^F|_{z=0+} \right) &= V d \zeta \Psi_{\sigma}^F|_{z=0+} \\ &+ \begin{bmatrix} \omega \cdot \hat{\sigma} & 0 \\ 0 & -\omega \cdot \hat{\sigma} \end{bmatrix} \Psi_{\sigma}^F|_{z=0+} \end{aligned} \quad (5)$$

where $\zeta = \text{diag}(1, 1, -1, -1)$. We describe our results in terms of the dimensionless barrier strength $Z = \frac{V d m}{\hbar^2 k_F}$, RSOI strength $\lambda_{rso} = \frac{2m\lambda}{\hbar^2}$ and spin polarization $P = \frac{\Delta_{xc}}{2E_F}$.

In presence of thermal gradient across the junction with no applied bias voltage, the electronic contribution to the normalized thermal conductance in terms of the scattering processes is given by^{9,37},

$$\kappa = \sum_{\sigma} \int_0^{\infty} \int_s \frac{d^2 k_{\parallel}}{2\pi k_F^2} [1 - R_{\sigma}^h - R_{\sigma}^e] \left[\frac{(E - E_F)^2}{k_B^2 T^2 \cosh^2 \left(\frac{E - E_F}{2k_B T} \right)} \right] dE \quad (6)$$

where the NR and AR probability can be defined as $R_{\sigma}^{e(h)}(E, k_{\parallel}) = \text{Re}[k_{\sigma}^{e(h)} |r_{\sigma}^{e(h)}|^2 + k_{-\sigma}^{e(h)} |r_{-\sigma}^{e(h)}|^2]$ satisfying the current conservation. Here, the integration with respect to k_{\parallel} is performed over the entire plane ($X - Y$)

of the interface. It is convenient to define a dimensionless wave vector $k = k_{||}/k_F$ and compute the integration in terms of it while calculating the TC. k_B is the Boltzmann constant. We consider the unit where $k_B = 1$. T is scaled by T_c , which is the critical temperature of the conventional singlet superconductor.

Within the linear response regime, we obtain the expression for the thermopower or SkC as follows⁴⁵,

$$S = - \left(\frac{V}{\delta T} \right)_{I=0} = - \frac{1}{eT} \frac{\alpha}{G} \quad (7)$$

where the thermoelectric-coefficient α and the electrical conductance G are represented as,

$$\alpha = \sum_{\sigma} \int_0^{\infty} \int_s \frac{d^2 k_{||}}{2\pi k_F^2} [1 - R_{\sigma}^h - R_{\sigma}^e] \left[\frac{(E - E_F)}{k_B T \cosh^2 \left(\frac{E - E_F}{2k_B T} \right)} \right] dE \quad (8)$$

and

$$G = \sum_{\sigma} \int_0^{\infty} \int_s \frac{d^2 k_{||}}{2\pi k_F^2} \frac{[1 + R_{\sigma}^h - R_{\sigma}^e]}{\left[k_B T \cosh^2 \left(\frac{E - E_F}{2k_B T} \right) \right]} dE \quad (9)$$

In terms of SkC, electrical conductance and thermal conductance the FOM zT is given by,

$$zT = \frac{S^2 GT}{K} \quad (10)$$

where $K = \kappa - \frac{\alpha^2}{TG}$. After applying the temperature difference between the two sides of the junction we obtain thermal current which essentially develops a voltage difference between them following the Peltier effect. This causes a correction to the thermal conductance as well. We consider such correction while defining the FOM of the system as every material manifesting Seebeck effect must exhibit the Peltier effect⁴⁶.

III. RESULTS AND DISCUSSION

In this section we present our numerical results for TC, SkC and FOM of the ferromagnet-superconductor junction, both in absence and presence of interfacial RSOI, in three different sub-sections. We discuss our results in terms of the scattering processes that occur at the interface of the FS hybrid structure and various parameters of the system.

A. Thermal conductance

In this subsection we present our results for the thermal conductance. In Fig. 3 we show the variation of thermal conductance κ as a function of temperature T/T_c in

absence of RSOI for various polarization strength P of the ferromagnet, starting from the unpolarized ($P = 0$) to the half-metallic ($P = 1$) limit. Fig. 3[(a), (b), (c) and (d)] correspond to the interfacial scalar barrier strength $Z = 0, 1, 2$ and 4 , respectively. From all the four figures it is apparent that TC increases exponentially with temperature. This behavior being independent of the barrier strength and polarization, is similar to the case of conventional normal metal-superconductor junction. The exponential nature of the thermal conductance arises due to the spherical symmetry of the s -wave superconductor^{8,47}. With the increase of temperature, the superconducting gap decreases resulting in reduction of AR amplitude and simultaneous increase of tunneling as electron like quasi-particles. Thermal resistance of the superconductor falls off exponentially as the temperature is increased⁴⁷. As a consequence, κ rises with the temperature following an exponential nature. However, the rate of increase of κ completely depends on the polarization P of the ferromagnet. Now gradual tunability of the polarization P does not ensure any monotonic behavior of the

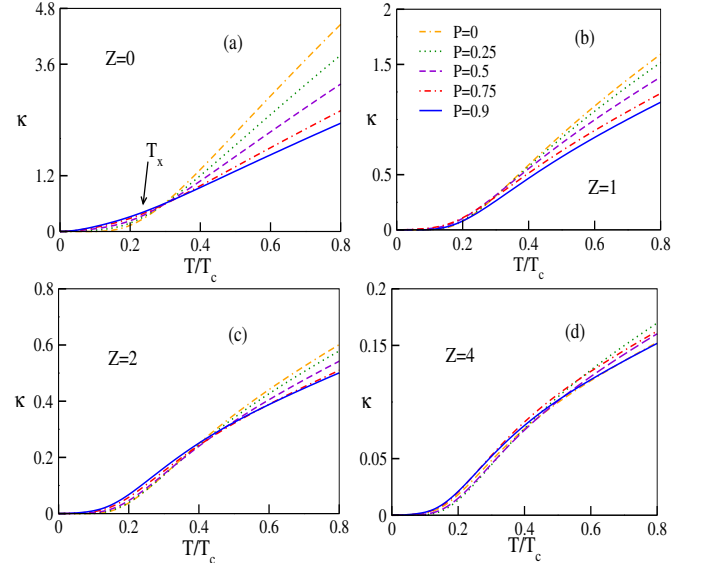


FIG. 3. (Color online) The behavior of thermal conductance (κ) is shown as a function of temperature (T/T_c) in absence of RSOI ($\lambda_{rso} = 0$) for different values of barrier strength (Z) and polarization (P) of the ferromagnet.

TC. It also depends on both the temperature and barrier strength. To illustrate this, we discuss the scenarios for different values of Z one by one. When $Z = 0$, the rate of increase of κ is very slow with the increase of polarization for a particular value of T/T_c (see Fig. 3(a)). This is true as long as $T/T_c < 0.3$. Whereas, for $T/T_c > 0.3$ the scenario becomes opposite *i.e.* κ starts decreasing with the change of polarization for a fixed T/T_c . There is a cross-over temperature T_x (~ 0.3 in this case) separating the two different behaviors of the TC with polarization. We explain this phenomenon as follows. For very low

T/T_c i.e. $T < T_x$, superconductor gap parameter does not change by appreciable amount. In this situation, increase of polarization causes reduction of AR due to minority spin sub-band. This results in enhancement of TC. Such enhancement is maximum in the half-metallic limit ($P = 1$) when AR vanishes due to the absence of minority spin-band. After a certain cross-over temperature, the gap decreases significantly with T/T_c and the tunneling increases accordingly as long as $T \simeq T_c$. On top of that, if we increase the polarization, tunneling due to the minor spin band also decreases leaving the major spin band contribution unchanged. As a whole, the change of behaviors of all the scattering processes results in reduction of TC with polarization in the high temperature regime ($T > T_x$).

Now let us consider finite Z at the interface. In presence of the barrier, incident electrons also encounter NR along with AR from the interface. NR reduces κ . Hence,

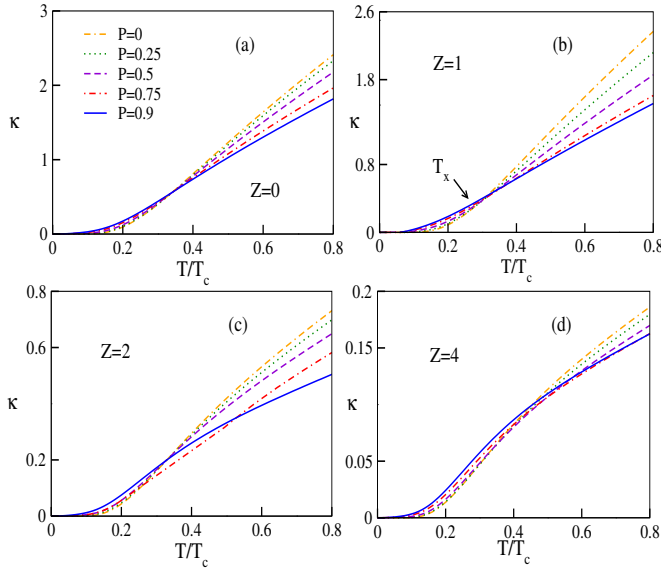


FIG. 4. (Color online) The variation of thermal conductance (κ) with respect to temperature (T/T_c) is depicted in presence of RSOI ($\lambda_{rso} = 2$) for different values of the barrier strength (Z) and polarization (P) of the ferromagnet.

the higher is the barrier strength Z the lower is κ for a particular temperature and polarization. This is apparent by comparing all the four figures of Fig. 3. The cross-over temperature T_x separating the behaviors of the TC with P , decreases as soon as we consider finite Z as depicted in Fig. 3(b). It becomes ~ 0.2 for $Z = 1$. However, T_x translates towards the high temperature limit with the increase of barrier strength (see Fig. 3(c) and (d)). For low Z , TC does not change by appreciable amount with the increase of P because of NR. In the low temperature regime, enhancement of P causes reduction of AR. This does not ensure the increase of TC as tunneling decreases due to the reflection from the interface. As Z is enhanced, NR starts dominating over the other

processes. This not only causes reduction of TC but also translates T_x towards the high temperature regime. For example, $T_x \sim 0.5$ (see Fig. 3(c)) and 0.8 (see Fig. 3(d)) for $Z = 2$ and $Z = 4$, respectively. Also, there is a tendency of saturation of κ when $T \rightarrow T_c$ irrespective of P for higher barrier strength associated with very small change of κ with P . For higher Z , AR, TE and TH are dominated by NR. Therefore, tuning polarization does not cause appreciable variation in the tunneling as well as AR resulting in very small change of TC leading towards its saturation.

Now we incorporate RSOI at the interface of the FS junction. In Fig. 4, we show the variation of the TC as a function of temperature (T/T_c) for finite RSOI strength. Here, Fig. 4[(a),(b),(c) and (d)] represent the scalar barrier strength $Z = 0, 1, 2$ and 4 , respectively. We begin our discussion on the effect of RSOI by considering the case of $Z = 0$. Comparing Fig. 3(a) and Fig. 4(a) we observe that in presence of finite RSOI, TC decreases irrespective of the value of the polarization. Ferromagnet-superconductor structure with $P = 0$ is exactly equivalent to a conventional normal metal-superconductor junction¹ for which the sub-gap contribution to κ is zero. The reason is that within the sub-gapped regime total AR probability is exactly equal to 1 i.e. $R_{\sigma}^h = 1$ with the reflection probability $R_{\sigma}^e = 0$ as $Z = 0$ ³⁷. Therefore, the sub-gap contribution to the TC is zero for this particular case. This is also evident from Eq. (6). Only quasi-particle tunneling contributes to the thermal conductance. Nevertheless, in presence of finite polarization of the ferromagnet the sub-gap contribution is finite. With the inclusion of interfacial RSOI, the spin-flip counter-parts of both types of scattering processes AR and tunneling as electron or hole like quasi-particles are possible to take place from the interface. The relative amplitudes corresponding to the spin-conserving and spin-flipping processes will be completely determined by the strength of RSOI. However, the behavior of the TC with the polarization and temperature remain qualitatively similar to that in absence of RSOI. Enhancement of polarization P indicates the minority of one spin sub-band with which AR probability decreases but SAR probability increases leaving the total AR probability 1 and thus maintaining the usual result for the sub-gapped energy regime. Whereas tunneling corresponding to the minor spin sub-band reduces. This effectively reduces κ by considerable amount (see Fig. 3(a) and Fig. 4(a) for comparison) as during the evaluation of κ , all the electrons corresponding to all the energy values are taken into account. Now incorporating finite barrier strength Z makes κ behave differently from the $Z = 0$ case [see Fig. 4(b)-(d)]. In presence of RSOI, interface barrier also causes SNR in addition to NR which effectively reduces the TC from the values in the previous case ($Z = 0$). Interplay of all these spin-conserving and spin-flipping scattering processes effectively increases the magnitude of κ . If we increase Z further, NR and SNR start dominating and as a result, κ decreases for a particular value of P and T/T_c . How-

ever, the scenario becomes much more interesting when we compare Fig. 3(b) and Fig. 4(b). Comparing these two figures we notice that in presence of RSOI, behavior of κ with RSOI is not monotonic. It is clear from the fact that for $Z = 1$, TC increases while we introduce RSOI at the interface. On the other hand for higher values of Z ($Z = 2$ and $Z = 4$), κ decreases with the incorporation

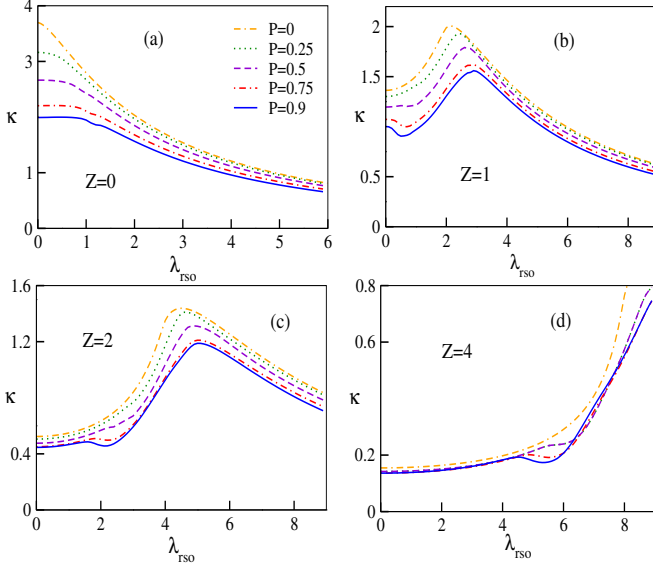


FIG. 5. The behavior of thermal conductance (κ) is displayed as a function of RSOI strength λ_{rso} for a particular temperature ($T/T_c = 0.7$) and different values of the barrier strength (Z) and polarization (P) of the ferromagnet.

of RSOI. It is evident from the comparison of Fig. 3 and Fig. 4 for all values of Z . Therefore, it is interesting to investigate the behavior of κ as a function of RSOI strength *i.e.* λ_{rso} in order to have a transparent picture. Note that, the cross-over temperature separating the two opposite behaviors of the TC with polarization also exists in presence of RSOI. Also the magnitude of T_x shifts towards the high temperature regime with the enhancement of Z as before.

For illustration, we present in Fig. 5 the variation of TC as a function of the RSOI strength for a particular temperature $T/T_c = 0.7$. Here, (a), (b), (c) and (d) represent different barrier strength, $Z = 0, 1, 2$ and 3 , respectively. In absence of scalar barrier ($Z = 0$), when we increase the RSOI strength TC monotonically decreases irrespective of the polarization (see Fig. 5(a)). In presence of RSOI, spin-flip AR takes place. As we increase λ_{rso} spin-flip counter part starts dominating. Hence, SAR becomes higher in magnitude with the enhancement of λ_{rso} . With the increase of SAR, κ decreases. Spin-flip counter parts of NR will also increase in this case but its effect on TC is less dominating compared to AR. As a consequence we get monotonically decreasing behavior of κ . Now with a particular RSOI strength, increasing polarization means reduction of AR keeping SAR almost

unaffected. Also, spin-flip tunneling decreases by negligible amount. This results in reduction of TC.

Comparing the magnitudes of κ corresponding to the four figures of Fig. 5 it is evident that introduction of finite barrier Z effectively reduces TC, being independent of the value of RSOI strength, due to the finite reflection from the barrier. In presence of barrier when we increase RSOI, initially κ does not show any appreciable change as long as λ_{rso} is very small compared to Z . If we gradually increase RSOI strength, TC exhibits non-monotonic behavior. κ increases gradually, attains a maxima and then again decreases with the increase of λ_{rso} as depicted in Fig. 5(b). The reason behind this non-monotonicity can be attributed to the interplay of all the six scattering processes occurring at the interface of FS structure. With the increase of λ_{rso} probabilities of all the spin-flip scattering processes increase. However, for a low barrier strength ($Z = 1$) SNR cannot dominate κ significantly compared to the spin-flip tunneling. Interplay of these processes results in enhancement of κ with the rise of λ_{rso} accordingly. For sufficiently higher λ_{rso} all the spin-flip processes start dominating over the spin-conserving processes. After a certain enhancement of RSOI, the probability of spin-flip scattering processes do not dominate further. Instead the spin-conserving scattering probabilities decrease with the increase of λ_{rso} . As a consequence, TC decreases. Behavior of κ with the change of polarization remains monotonically decreasing similar to the case before.

If we further increase Z , κ maintains its non-monotonic behavior with the rise of RSOI strength. However, the maxima moves towards the higher value of λ_{rso} . To illustrate this, we refer to Fig. 5(c) and (d). For higher values of Z , magnitudes of κ decreases as SNR and NR starts dominating. In this situation to obtain the maxima of κ we have to tune RSOI strength accordingly. This results in shifting of the peaks of κ towards higher λ_{rso} .

Note that, we present our results of κ as a function of λ_{rso} for $T/T_c = 0.7$. If we consider the low temperature regime, particularly lower than the cross-over value T_x , we expect similar non-monotonic behavior of the TC with RSOI strength. Only change lies into the nature of κ with polarization at a particular RSOI strength following the above discussion. That means κ will rise with the increase of P for fixed RSOI. For very low temperature such as $T/T_c \sim 0.1$, the amount of change in magnitude of the TC is vanishingly small.

So far, we have not discussed about the orientation of the magnetization. We present all of our results for $\theta = \pi/2$ and $\phi = 0$. Very recently, Högl *et al.* have revealed the fact that electronic conductance shows an anisotropy with the rotation of the magnetization \mathbf{m} ³¹. However, in case of thermal transport, contributions from all the energy values are taken into consideration. Therefore, with the change of \mathbf{m} there is no appreciable change in thermal conductance as all contributions due to different orientations of \mathbf{m} are averaged out during integration over the energy (see Eq. (6)). This fact remains un-

changed for any temperature ($T < T_c$) and polarization P .

B. Seebeck co-efficient

In this sub-section we study the phenomenon of Seebeck effect which is a direct measure of the local thermoelectric response. The behavior of SkC as a function of temperature and RSOI for different values of P and Z are presented. All the results, we have presented here, correspond to the particular orientation of the magnetization vector as mentioned in the previous sub-section.

In Fig. 6[(a), (b), (c) and (d)], we illustrate the behavior of S as a function of T/T_c corresponding to the scalar barrier potential $Z = 0, 1, 2$ and 4 , respectively. From all the four figures it is clear that SkC is negative throughout the window for all values of Z irrespective of the polarization of the ferromagnet. It is solely due to

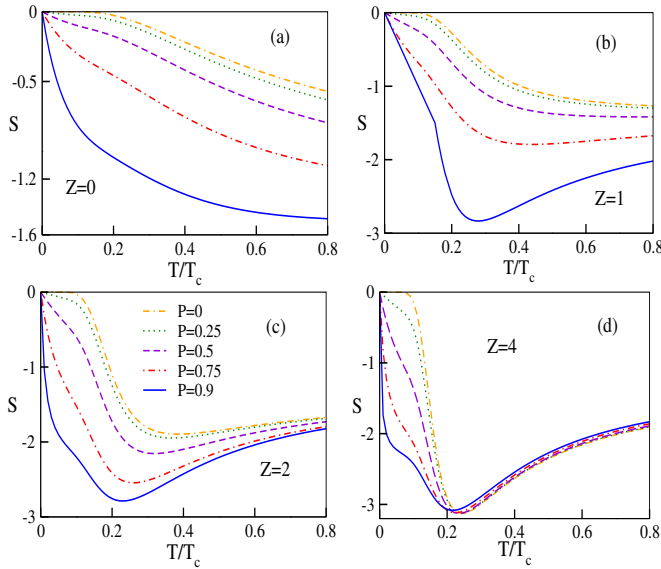


FIG. 6. (Color online) The behavior of Seebeck co-efficient (S) is shown as a function of temperature (T/T_c) in absence of RSOI ($\lambda_{rso} = 0$) for different values of the barrier strength (Z) and polarization (P) of the ferromagnet.

the contributions arising from the electrons. So, we discuss only the magnitude of the SkC throughout the rest of the manuscript. SkC increases with T/T_c in absence of the barrier *i.e.* $Z = 0$. This phenomenon is true for all values of the polarization P . While for a particular value of temperature, it also increases with the increase of P . We can explain this phenomenon as follows. For $Z = 0$, the probability of NR is zero. With the increase of temperature, superconducting gap decreases minimizing the phenomenon of AR to occur. This results in enhancement of transmission of energy with temperature. It is also evident from the expression of SkC (see Eq. (7)). Hence, we can say that reduction of R_g^h causes enhance-

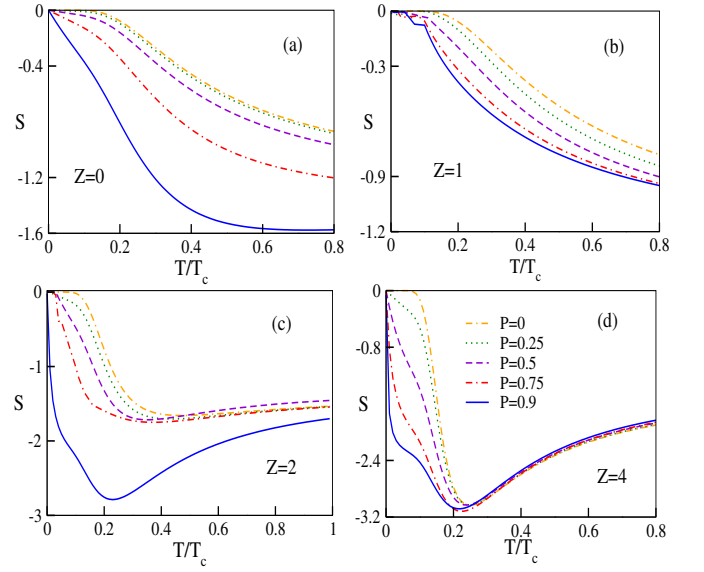


FIG. 7. (Color online) The variation of Seebeck co-efficient (S) with respect to temperature (T/T_c) is displayed in presence of RSOI ($\lambda_{rso} = 2$) for different values of barrier strength (Z) and polarization (P) of the ferromagnet.

ment of the magnitude of the numerator in Eq. (7). The latter essentially describes the thermal co-efficient. At the same time denominator or the electronic conductance decreases. This effectively enhances SkC magnitude. In fact, for the sub-gapped energy regime we have always zero thermal co-efficient resulting in vanishing contribution to the SkC. There are finite contributions arising only from the energy regime above the gap.

Now we consider finite barrier strength at the junction. In presence of finite Z , thermopower increases monotonically for low values of P . The amount of enhancement is higher for the higher values of P . However there is a smooth transition from monotonic to non-monotonic behavior of SkC with temperature as the polarization tends to the half-metallic limit *i.e.* $P = 1$. It initially rises with T/T_c and then decreases in high temperature regime with an extremum in the Seebeck profile. According to the definition we can describe this feature of SkC in terms of α and G . In presence of finite Z , NR reduces both α and G . Now change of SkC occurs depending on their relative magnitudes. As a consequence, S increases in presence of finite Z in comparison to the case for $Z = 0$ (comparing Figs. 6(a) and (b)). Moreover, there is a tendency of saturation of the thermopower magnitude in the higher temperature regime irrespective of the values of P . For $Z = 1$, it is more clear for higher values of P . For sufficiently higher temperature the gap reduces significantly resulting in enhancement of conductance. However, for higher polarization, G does not increase with T/T_c by appreciable amount after a certain temperature due to the absence of minority spin band. As a consequence, SkC decreases resulting in a non-monotonic behavior es-

pecially for higher polarization. Such non-monotonicity is much more pronounced for higher values of Z (see Fig. 6(c) and (d)). Also, the saturation regime reaches faster for higher Z with the enhanced NR. For higher barrier strength, SkC changes by very small amount with Z for a particular P and T/T_c due to the suppression of all other scattering processes by NR.

Furthermore, we investigate what happens to SkC when RSOI is taken into account at the interfacial layer. In Fig. 7 we display the behaviors of SkC with T/T_c

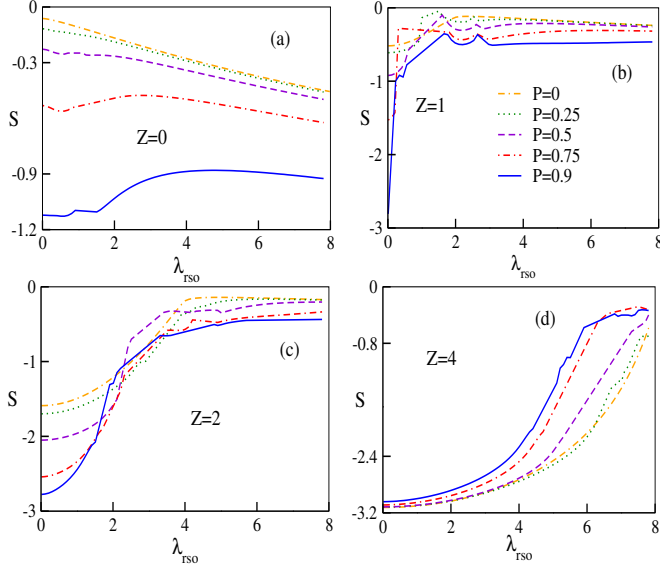


FIG. 8. (Color online) The behavior of Seebeck co-efficient (S), at temperature $T/T_c = 0.5$, is shown as a function of RSOI strength (λ_{rso}) for different values of barrier strength (Z) and polarization (P) of the ferromagnet.

for both in absence and presence of finite barrier strength considering different values of polarization. Here, (a), (b), (c) and (d) represent $Z = 0, 1, 2$ and 4 , respectively similar to the previous figures. Comparing Fig. 6(a) and Fig. 7(a), it is clear that for $Z = 0$ the nature of the curves for S vs. T/T_c in absence and presence of RSOI are quite similar to each other except the slopes. Note that, SkC changes much faster with T/T_c in presence of RSOI. It also increases with the change of polarization P at a particular temperature. However, the features of SkC changes significantly when we incorporate barrier strength at the FS interface. For low Z (for *e.g.* $Z = 1$), SkC gets reduced as soon as we incorporate RSOI at the interface (compare Figs. 6(b) and 7(b)). This happens completely due to the presence of spin-flip scatterings at the junction of the hybrid structure like SNR, SAR. Their competition ultimately reduces G much faster compared to α . This causes reduction of Seebeck voltage across the junction. However, we recover the non-monotonic behavior of SkC when Z becomes high ($Z = 2$ and 4) as demonstrated in Figs. 7(c) and (d). For higher barrier strength, S does not change by appreciable amount

in presence of RSOI in comparison to that in absence of RSOI. This is true for all values of P . The change of SkC with the rise of polarization is also very small in presence of RSOI similar to the case in absence of RSOI. This phenomenon can be explained as follows. For higher barrier strength NR and SNR dominate over all other scattering processes. Hence, both α and G get reduced by some amounts which are comparable to each other.

To understand the role of RSOI in more detail, we illustrate the behavior of SkC (S) with respect to RSOI (λ_{rso}) for a fixed value of temperature $T/T_c = 0.5$ in Fig 8[(a), (b), (c) and (d)] for four different values of the barrier strength as before. For $Z = 0$, behavior of SkC with λ_{rso} are different for different P . For zero or lower values of polarization, it rises with the increase of RSOI strength. The rate of increase, however, changes when P becomes high. There is a transition from increasing to decreasing nature of S vs. λ_{rso} curves with the increase of polarization. As soon as we incorporate Z , the situation changes dramatically. SkC sharply falls with the temperature in presence of barrier strength due to the large boosts of NR and SNR scattering phenomenon. The rate of decrease of SkC becomes lower with the increase of barrier strength. With very high RSOI it becomes saturated with the saturation region shifts towards the higher RSOI strength as one increases the barrier strength Z . This is clear by comparing Figs. 8[(b)-(d)]. Most interestingly, we ob-

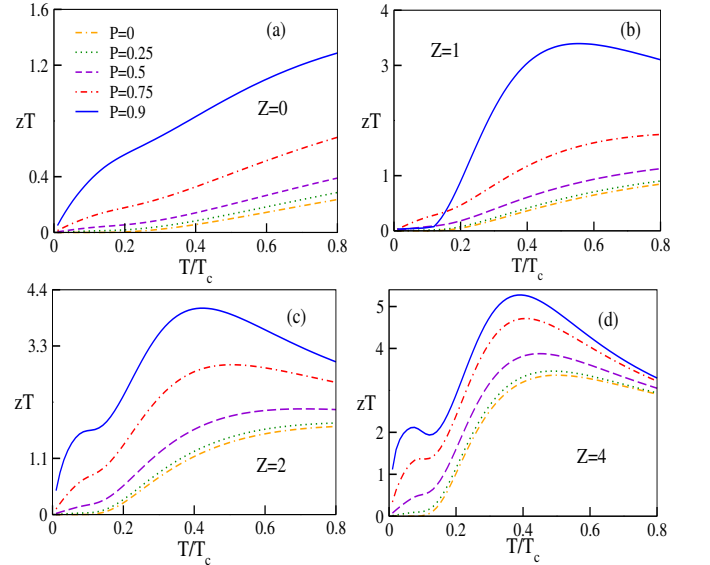


FIG. 9. (Color online) The feature of Figure of merit (zT) is depicted as a function of temperature (T/T_c) in absence of RSOI ($\lambda_{rso} = 0$) for different values of barrier strength (Z) and polarization (P) of the ferromagnet.

serve that for finite and low value of Z , SkC always increases with polarization for all values of λ_{rso} . On the contrary, for higher Z (*e.g.* $Z = 4$) we obtain exactly opposite scenario where S decreases with the increase of P . There is a transition of the behavior of the SkC with the

polarization at some certain strength of Z . However, it is always possible to obtain large thermopower in presence of low RSOI strength for all values of polarization.

C. Figure of merit (zT)

In order to understand the efficiency of our FS junction as a thermo-electric material, in this sub-section, we explore the behavior of FOM both in presence and absence of RSOI.

In Fig. 9 we display the variation of zT with respect to T/T_c for various polarization and barrier strength. Here, (a), (b), (c) and (d) represent the same parameter values as mentioned in the previous cases. The value of zT is very small for $P = 0$ and in the absence of barrier (see Fig. 9(a)). However, it increases with the increase of polarization as well as temperature. We can obtain FOM ~ 1.3 when the polarization of the ferromagnet tends to half-metallic limit ($P = 1$). The rate of increase of zT with P , for a particular temperature, increases with the increase of polarization of the ferromagnet. In general, FOM can be defined in terms of the three parameters namely thermal co-efficient, SkC and electronic conductance as well (see Eq. (10)). The nature of FOM, whether it is increasing or decreasing, completely depends on their relative magnitudes. Similar enhancement of zT has also been proposed in literature by tuning exchange field². Search for FOM more than 1 in order to have an efficient thermoelectric material has always remained in the focus of material science. In our case FOM can also be enhanced not only by tuning the polarization P but also setting finite barrier potential at the junction as shown in Figs 9[(b)-(d)]. For higher values of Z , the behavior of zT becomes non-monotonic. It initially rises with the temperature and after a certain temperature it decreases.

In order to investigate the effect of interfacial RSOI on the FOM, we show zT as a function of T/T_c in Fig. 10 for $\lambda_{rso} = 2$. In absence of any barrier at the interface, FOM increases with the rise of temperature, for a particular value of polarization. The behavior of zT with temperature and also with polarization is very much similar to that in absence of RSOI which becomes clear by comparing Fig. 9(a) and Fig. 10(a). However the scenario changes drastically when we consider low but finite barrier at the junction. As mentioned earlier, presence of RSOI with small λ_{rso} induces spin-flip scattering process which reduces the SkC and enhances thermal conductance at the same time. Also, the electronic conductance increases by small amount as shown in Ref. 31. Their relative magnitudes result in high reduction of zT for all values of P as shown in Fig. 10(b). Moreover, the variation of zT is very small with the change of polarization. This phenomenon is true for low barrier strength. For higher barrier strength, exactly opposite phenomenon occurs. Their relative magnitudes cause enhancement of zT with the increase of Z for the weak strength of RSOI (λ_{rso}). Therefore, we can say that FOM can be enhanced

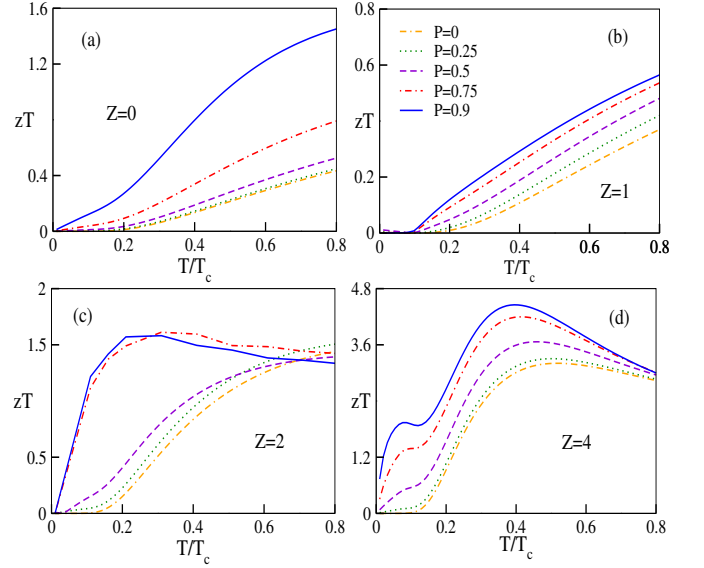


FIG. 10. (Color online) The variation of Figure of merit (zT) is shown as a function of temperature (T/T_c) in presence of finite RSOI ($\lambda_{rso} = 2$) for different values of barrier strength (Z) and polarization (P) of the ferromagnet.

by increasing any one of the parameters *i.e.* polarization, barrier strength and temperature keeping the other two fixed both in absence and presence of RSOI at the in-

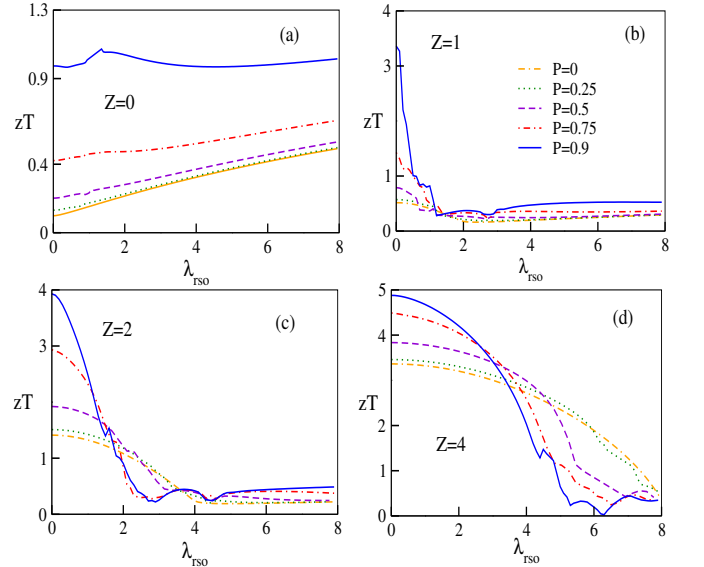


FIG. 11. (Color online) The behavior of Figure of merit (zT) is illustrated as a function of RSOI strength (λ_{rso}) at $T/T_c = 0.5$ for different values of the barrier strength (Z) and polarization (P) of the ferromagnet.

terfacial layer of our FS junction. Note that, all these phenomena are true for weak Rashba interaction.

We demonstrate the behavior of zT as a function of

λ_{rso} in Fig. 11 where (a)-(d) correspond to the same values of Z as in the previous figures. In absence of any barrier ($Z = 0$) and for low polarization of the ferromagnet, zT rises with the enhancement of λ_{rso} almost linearly. Such linear behavior changes when the polarization of the ferromagnet is considered towards the half-metal one *i.e.* $P = 1$. For a particular choice of λ_{rso} , FOM increases with the increase of polarization too as in absence of RSOI. This scenario reverses its character in presence of low Z . Under such circumstances, zT falls off rapidly with the increase of λ_{rso} . When we further increase Z , the behavior of zT changes slowly with the RSOI strength. Depending on the value of Z , (see Figs. 11(c) and (d)) FOM can even reach the value ~ 5 by using half-metal for weak or moderate RSOI. After a critical Rashba strength it falls off rapidly and becomes vanishingly small. However, the critical value of Rashba strength translates towards the higher regime with the increase of Z .

IV. SUMMARY AND CONCLUSIONS

To summarize, in this article, we have investigated thermo electric properties of a ferromagnet-superconductor junction driven by a thermal gradient. At the interfacial layer we have incorporated RSOI along with scalar potential barrier. We have analyzed our results for the thermal conductance, Seebeck co-efficient and figure of merit as a function of temperature, polarization of the ferromagnet and RSOI strength. Thermal conductance κ exhibits exponential rise with temperature following the s -wave symmetry. We have observed a cross-over temperature T_x separating the two different regimes corresponding to opposite behaviors of κ with the polarization of the ferromagnet. Below the cross-over temperature, κ increases with the increase of polarization whereas for all the temperatures above the cross-over temperature it decreases with polarization. This phenomenon is true both in absence and presence of barrier strength. With the increase of barrier strength the cross-over temperature moves towards the higher temperature value. Inclusion of interfacial Rashba spin-orbit field causes reduction of thermal conductance due to the appearance of spin-flipped SAR process, in absence of any barrier. On the other hand, interfacial RSOI can enhance the TC in presence of finite barrier due to the interplay of both. We have obtained a non-monotonic behavior of the thermal conductance κ as we vary the interfacial RSOI strength. Although the corresponding maxima of κ moves towards the critical temperature T_c with the enhancement of barrier strength Z . Throughout the manuscript we have considered only the electronic contribution to the TC neglecting the contribution due to phonons which is a valid approximation for low temperature gradient.

We have also investigated the Seebeck co-efficient in absence and presence of interfacial RSOI and scalar barrier. It can be enhanced by using ferromagnet with higher

polarization and by increasing the temperature (below the critical temperature T_c) as well. A non-linear behavior of the SkC with the temperature can be obtained in presence of barrier potential at the junction. Whereas presence of RSOI can reduce or enhance it depending on the barrier strength. For low barrier strength, SkC increases with the increase of polarization. However, an exactly opposite behavior is observed when barrier strength becomes high.

To quantify the thermoelectric power efficiency of the FS structure, we as well as compute the figure of merit zT both in presence and absence of RSOI and scalar potential barrier. We show that the FOM can be enhanced to more than 1 by setting the polarization of the ferromagnet very high (towards the half-metallic limit). It can further be enhanced by considering finite potential barrier at the junction. In particular, the higher the barrier strength the higher the FOM turns out to be. While, inclusion of RSOI can reduce it for low barrier strength. In contrast, for higher barrier strength, value of zT can again be more than 1 ($zT \sim 4 - 5$) depending on the polarization of the ferromagnet. These phenomena comes out to be valid for weak Rashba spin-orbit interaction. Presence of strong RSOI can highly reduce it irrespective of the strength of the barrier potential.

As far as the practical realization of our model is concerned, it may be possible to fabricate such a FS hybrid structure by growing thin layers of a spin singlet superconductor (e.g. Nb material) and a ferromagnetic insulator (EuO)^{48,49} on top of each other. To design the interfacial layer, responsible for the spin-orbit field, one can use a thin layer of zinc-blende semiconductor⁵⁰. A very thin layer is to be deposited in order to create the barrier. An additional gate voltage can be implemented to create the scalar potential barrier at the interface. The magnetization vector of the ferromagnet can be rotated by some external magnetic field. Additional effects of such external field can be avoided by using dysprosium magnets³¹. Also, from an experimental point of view, the polarization of the ferromagnet can be a more controllable parameter than the interfacial RSOI strength. For a typical s -wave superconductor, for *e.g.* Nb with $T_c = 9.3$ K ($\Delta_s \sim 3$ meV), to attain $zT \sim 4.5$ one needs a ferromagnetic exchange coupling $\Delta_{xc} \sim 0.6$ eV^{51,52}, temperature $T \sim 4$ K, interfacial Rashba parameter $\sim 60 - 80$ meV $\cdot \text{\AA}$ ⁵³ and a scalar potential barrier with height $V \sim 0.5$ eV and width $d \sim 2 - 4$ nm⁵⁴.

ACKNOWLEDGMENTS

PD thanks Department of Science and Technology (DST), India for the financial support through SERB NPDF (File no. PDF/2016/001178). We acknowledge S. D. Mahanti for helpful discussions and encouragement. AMJ also thanks DST, India for financial support. Finally, we acknowledge Indian citizens for supporting research in basic science.

-
- * paramitad@iopb.res.in
† arijit@iopb.res.in
‡ jayan@iopb.res.in
- ¹ V. Chandrasekhar, Superconductor Science and Technology **22**, 083001 (2009).
 - ² P. Machon, M. Eschrig, and W. Belzig, New J. Phys. **16**, 073002 (2014).
 - ³ A. Ozaeta, P. Virtanen, F. Bergeret, and T. Heikkilä, Phys. Rev. Lett. **112**, 057001 (2014).
 - ⁴ M. S. Kalenkov, A. D. Zaikin, and L. S. Kuzmin, Phys. Rev. Lett. **109**, 147004 (2012).
 - ⁵ P. Machon, M. Eschrig, and W. Belzig, Phys. Rev. Lett. **110**, 047002 (2013).
 - ⁶ S. Kolenda, M. J. Wolf, and D. Beckmann, Phys. Rev. Lett. **116**, 097001 (2016).
 - ⁷ S. Kolenda, P. Machon, D. Beckmann, and W. Belzig, Beilstein J. Nanotechnol. **7**, 1579 (2016).
 - ⁸ A. F. Andreev, Zh. Eksp. Teor. Fiz. **46**, 1823 (1964).
 - ⁹ T. Yokoyama, J. Linder, and A. Sudbø, Phys. Rev. B **77**, 132503 (2008).
 - ¹⁰ R. Beiranvand and H. Hamzehpour, arXiv:1612.01461.
 - ¹¹ M. Alomar and D. Sánchez, Phys. Rev. B **89**, 115422 (2014).
 - ¹² S. J. Blundell and K. M. Blundell, *Concepts in thermal physics* (OUP Oxford, 2009).
 - ¹³ S.-Y. Hwang, R. Lopez, and D. Sanchez, Phys. Rev. B **94**, 054506 (2016).
 - ¹⁴ G. J. Snyder and E. S. Toberer, Nat. Mater. **7**, 105 (2008).
 - ¹⁵ H. Sevinçli and G. Cuniberti, Phys. Rev. B **81**, 113401 (2010).
 - ¹⁶ M. Zabarjadi, K. Esfarjani, M. Dresselhaus, Z. Ren, and G. Chen, Energy & Environmental Science **5**, 5147 (2012).
 - ¹⁷ F. Giazotto, T. T. Heikkilä, A. Luukanen, A. M. Savin, and J. P. Pekola, Rev. Mod. Phys. **78**, 217 (2006).
 - ¹⁸ H. Goldsmid, *Electronic Refrigeration* (Pion, London, 1986), Vol. 3, pp. 57–87.
 - ¹⁹ Y. Xu, Z. Gan, and S.-C. Zhang, Phys. Rev. Lett. **112**, 226801 (2014).
 - ²⁰ J. Liu, Q.-f. Sun, and X. Xie, Phys. Rev. B **81**, 245323 (2010).
 - ²¹ D. Dragoman and M. Dragoman, Appl. Phys. Lett. **91**, 203116 (2007).
 - ²² H. Ohta, S. Kim, Y. Mune, T. Mizoguchi, K. Nomura, S. Ohta, T. Nomura, Y. Nakanishi, Y. Ikuhara, M. Hirano, *et al.*, Nat. Mater. **6**, 129 (2007).
 - ²³ J. Linder and M. E. Bathen, Phys. Rev. B **93**, 224509 (2016).
 - ²⁴ M. E. Bathen and J. Linder, arXiv:1608.06285.
 - ²⁵ J. Linder and A. Sudbø, Phys. Rev. B **76**, 214508 (2007).
 - ²⁶ S.-Y. Hwang, R. Lopez, and D. Sanchez, Phys. Rev. B **94**, 054506 (2016).
 - ²⁷ M. Alidoust, G. Rashedi, J. Linder, and A. Sudbø, Phys. Rev. B **82**, 014532 (2010).
 - ²⁸ E. Zhao, T. Löfwander, and J. Sauls, Phys. Rev. Lett. **91**, 077003 (2003).
 - ²⁹ J. Peltonen, P. Virtanen, M. Meschke, J. Koski, T. Heikkilä, and J. P. Pekola, Phys. Rev. Lett. **105**, 097004 (2010).
 - ³⁰ S. Datta and B. Das, Appl. Phys. Lett. **56**, 665 (1990).
 - ³¹ P. Högl, A. Matos-Abiague, I. Žutić, and J. Fabian, Phys. Rev. Lett. **115**, 116601 (2015).
 - ³² A. Costa, P. Högl, and J. Fabian, Phys. Rev. B **95**, 024514 (2017).
 - ³³ E. I. Rashba, Physica E **34**, 31 (2006).
 - ³⁴ Y. A. Bychkov and E. I. Rashba, J. Phys. C: Solid State Phys. **17**, 6039 (1984).
 - ³⁵ K. Sun and N. Shah, Phys. Rev. B **91**, 144508 (2015).
 - ³⁶ I. Zutik, J. Fabian, and S. D. Sharma, Rev. Mod. Phys. **76**, 323 (2004).
 - ³⁷ G. E. Blonder, M. Tinkham, and T. M. Klapwijk, Phys. Rev. B **25**, 4515 (1982).
 - ³⁸ I. Žutić and O. T. Valls, Phys. Rev. B **61**, 1555 (2000).
 - ³⁹ P.-G. De Gennes, *Superconductivity of metals and alloys (advanced book classics)* (Perseus Books Group, 1999).
 - ⁴⁰ E. C. Stoner, Proc. R. Soc. A **169**, 339 (1939).
 - ⁴¹ A. Matos-Abiague, M. Gmitra, and J. Fabian, Phys. Rev. B **80**, 045312 (2009).
 - ⁴² M. De Jong and C. Beenakker, Phys. Rev. Lett. **74**, 1657 (1995).
 - ⁴³ X. Cao, Y. Shi, X. Song, S. Zhou, and H. Chen, Phys. Rev. B **70**, 235341 (2004).
 - ⁴⁴ M. Eschrig, Phys. Today **64**, 43 (2011).
 - ⁴⁵ M. Wysokiński, Acta Phys. Polo. A **122** (2012).
 - ⁴⁶ A. Bardas and D. Averin, Phys. Rev. B **52**, 12873 (1995).
 - ⁴⁷ A. F. Andreev, Sov. Phys. JETP **19**, 1228 (1964).
 - ⁴⁸ B. Matthias, R. Bozorth, and J. Van Vleck, Phys. Rev. Lett. **7**, 160 (1961).
 - ⁴⁹ T. Tokuyasu, J. Sauls, and D. Rainer, Phys. Rev. B **38**, 8823 (1988).
 - ⁵⁰ M. Deng, C. Yu, G. Huang, M. Larsson, P. Caroff, and H. Xu, Nano Lett. **12**, 6414 (2012).
 - ⁵¹ P. G. Steeneken, L. H. Tjeng, I. Elfimov, G. A. Sawatzky, G. Ghiringhelli, N. B. Brookes, and D. J. Huang, Phys. Rev. Lett. **88**, 047201 (2002).
 - ⁵² T. S. Santos and J. S. Moodera, Phys. Rev. B **69**, 241203(R) (2004).
 - ⁵³ A. Manchon, H. C. Koo, J. Nitta, S. M. Frolov, and R. A. Duine, Nat. Mater. **14**, 871 (2015).
 - ⁵⁴ S. M. Huang, A. O. Badrutdinov, L. Serra, T. Kodera, T. Nakaoka, N. Kumagai, Y. Arakawa, D. A. Tayurskii, K. Kono, and K. Ono, Phys. Rev. B **84**, 085325 (2011).